


ORIGINAL ARTICLE

Open Access



Evaluation of contrast-induced acute kidney injury using IVIM and DKI MRI in a rat model of diabetic nephropathy

Hongyan Dai^{1†}, Chun Zhao^{1†}, Yuxin Xiong², Qian He¹, Wei Su¹, Jianbo Li¹, Ying Yang², Ruyun Lin³, Shutian Xiang^{1*} and Juwei Shao^{1*} 

Abstract

Objective: To assess the potential of intravoxel incoherent motion (IVIM) and diffusion kurtosis imaging (DKI) in monitoring renal changes in a diabetic nephropathy (DN) rat model with acute kidney injury (CI-AKI) induced by iso-osmotic contrast media (IOCM) and low-osmotic contrast media (LOCM).

Methods: A diabetic nephropathy rat model was established, and the animals were randomly split into the LOCM group and IOCM group ($n = 13$ per group), with iopamidol and iodixanol injection, respectively (4 g iodine/kg). MRI including IVIM and DKI was performed 24 h before contrast medium injections (baseline) and 1, 24, 48, and 72 h after injections. Changes in pure molecular diffusion (D), pseudo-diffusion coefficient (D^*), perfusion fraction (f), mean diffusion (MD), mean kurtosis (MK), serum creatinine (SCr) and urea nitrogen (BUN), histopathology alterations, and α -smooth muscle actin (α -SMA) expression were assessed. Inter-observer agreement was evaluated using the intra-class correlation coefficient (ICC).

Results: Compared against baseline levels, significant decreases in D , D^* , and f were observed in all anatomical kidney compartments after contrast injection ($p < 0.05$). MD in the cortex (CO) and outer medullary (OM) gradually decreased, and MK in OM gradually increased 24–72 h after injection. D , D^* , f , and MD were negatively correlated with the histopathologic findings and α -smooth muscle actin (α -SMA) expression in all anatomical kidney compartments. Inter-observer reproducibility was generally good (ICCs ranging from 0.776 to 0.979).

Conclusions: IVIM and DKI provided noninvasive imaging parameters, which might offer effective detection of CI-AKI in DN.

Keywords: Contrast-induced acute kidney injury, Diabetic nephropathy, Iodinated contrast media, Intravoxel incoherent motion, Diffusion kurtosis imaging

Key points

- Nephrotoxicity of IOCM was lower than that of LOCM for diabetic nephropathy rats.
- IVIM and DKI noninvasively detected kidney damage after CI-AKI.
- Functional MRI manifestations were correlated with histopathology findings and α -SMA expression.

[†]Hongyan Dai and Chun Zhao have contributed equally to this work and are considered co-first authors

*Correspondence: xiangshutian@sina.com; wavevivi@163.com

¹ Department of Radiology, The Affiliated Hospital of Yunnan University, NO.176 Qingnian Road, Kunming 650021, Yunnan, China
Full list of author information is available at the end of the article

Background

Contrast-induced acute kidney injury (CI-AKI) is a frequently encountered global health problem [1, 2]. Contrast agent-associated acute renal failure is considered one of the most severe complications of CI-AKI [2], and its treatment is very costly. In addition, diabetic nephropathy (DN) as an irreversible disorder is a high-risk factor for CI-AKI [3–5]. Therefore, for DN patients, how to choose the type of contrast agent is particularly important.

At present, the pathogenesis of CI-AKI has not been fully revealed. Serum creatinine (SCr) is the primary parameter used for clinical evaluation of renal function, but it is not sufficiently sensitive to accurately assess the severity and progression of kidney disease [6].

A growing number of noninvasive and non-radiative magnetic resonance imaging (MRI) techniques without utilizing gadolinium contrast media have been applied in diagnosing renal diseases, including intravoxel incoherent motion (IVIM) and diffusion kurtosis imaging (DKI). IVIM estimates tissue microcapillary perfusion by bi-exponential fitting of multi-b-value DWI. As a result, it provides both pure diffusion and pseudo-diffusion (tissue perfusion) information. IVIM assesses renal pathological changes, microcirculatory perfusion, and humoral changes. Liang et al. adopted IVIM to longitudinally observe SD rats with CI-AKI [7]. The changes in D , D^* , and f occurred much earlier than SCr change, which was inconsistent with blood biochemistry results. This indicated that IVIM parameters were sensitive indicators of renal microstructure changes. Wang et al. longitudinally observed a rabbit CI-AKI model using IVIM [8]. It was found that there was a good correlation of histological score with D and f values. As a new technology, DKI based on non-Gaussian model yields an ultra-high b value (> 1000 s/mm²). It quantifies the size and direction of water molecule diffusion in tissues, reflects the microstructure of living body [9], and predicts renal damages [10, 11]. Previous studies have shown that DKI can be used to detect the degree of renal fibrosis in patients with IgA nephropathy and diabetic nephropathy [10, 11]. These findings indicated that the renal mean kurtosis (MK) increased with the deterioration of renal function and the progression of renal fibrosis. At present, there is few research on the application of DKI to detect CI-AKI.

This study intended to compare the effects of low- and iso-osmolar contrast media (LOCM and IOCM) on water diffusion, perfusion, and microstructure within renal tissue of DN rats following CI-AKI. Furthermore, we aimed to examine whether IVIM and DKI imaging could non-invasively detect these changes, which were verified by renal pathology and histological α -smooth muscle actin (α -SMA) expression.

Materials and methods

Animal model

Ethics approval was obtained from the local hospital ethics committee ((Ethics Committee of Affiliated Hospital of Yunnan University, China).

Twenty-six male Sprague–Dawley (SD) rats (certificate o. SCXK 2015-0002; Kunming, China) weighing 200–250 g were fed a high-fat diet (HFD). Citrate buffer with pH 4.5 was prepared by mixing citric acid and trisodium citrate (0.1 mol/l). Streptozocin (STZ, Sigma-Aldrich, St Louis, MO, USA) solution (3%) was prepared by dissolving 3 mg of STZ in 1 mL of citrate buffer (pH 4.5). After animals were fed with HFD for 21 days, STZ was injected intraperitoneally at doses of 20, 10, and 5 mg/kg/d on the 1st, 3rd, and 5th day, respectively. In addition, 20, 10, 5 mg/kg/d STZ was injected again on the 21st, 23rd, and 25th day, respectively, to induce diabetes in rats [12]. Blood was collected from the rat caudal vein and glucose level was measured. Diabetes in rats was confirmed with a fasting blood glucose (FBG) level of ≥ 16.7 mmol/L. After 6–8 weeks, 24-h urine was collected, and urinary albumin level was determined by the Albumin rat ELISA kit (Sigma), and urinary creatinine level was measured by the picrate method. Combined level of urinary albumin and creatinine was measured to determine whether the DN model was successfully established.

Experimental groups and procedures

Rats were randomly divided into two groups: LOCM ($n=13$) and IOCM ($n=13$). Contrast media were preheated to 37–38 °C, and the two groups of rat were injected with iopamidol-370 and iodixanol-320 (4 g iodine/kg) via the tail vein, respectively. For the control group, rats received the same volume of normal saline injection (i.e., baseline, total 26 rats).

Biochemistry assessment and histological analysis

Intracardiac blood was withdrawn from rats immediately after MRI scan to examine the renal function indexes, including concentrations of serum creatinine (SCr) and blood urea nitrogen (BUN). Three rats, selected randomly from the two groups, were killed at specific time points (baseline, 1, 24, 48, and 72 h after the injection). Hematoxylin and eosin (H&E) staining and immunohistochemical staining for α -SMA were performed, and the data were assessed by two senior pathologists (with more than 10 years of pathological diagnostic experience). Renal tissue damage was determined using the following scale [13]: injury limited to the glomerular structure (0–1.0), injury extending to the tubule cells (1.1–2.0), and injury including expansion and congestion of the

capillaries (2.1–3.0). Immunohistochemical staining for α -SMA was quantified using the Image J software (NIH, Bethesda, MD, USA).

MRI protocol

MRI was performed with a 3.0 Tesla scanner (Philips Ingenia, Best, The Netherlands) equipped with a 16-channel (CG-MUC49-H3000-AP) abdominal phased-array surface coil for signal reception (Chenguang Medical Technology Co., Ltd, Shanghai, China). After 8-h fasting, rats were anesthetized with intraperitoneal injection of 10% chloral hydrate (3.0 mL/kg) and immediately scanned in a head-first prone position. Abdomen of rat was bandaged to reduce the respiratory artifacts during MRI scan. MRI scanning was performed before injection and 1, 24, 48, and 72 h after administration of contrast agents, and pre-injection data were used as baseline values (Fig. 1). MRI sequences applied included axial T2-weighted imaging, axial IVIM, and axial DKI (Fig. 2).

IVIM adopted the following parameters: repetition time (TR)/echo time (TE), 1262/94 ms; slice thickness/gap, 2.0/0.5 mm; matrix, 110 × 110; field of view (FOV), 24 × 24 cm²; and nine *b* values, 0, 20, 50, 80, 100, 200, 400, 600, and 800 s/mm².

DKI was acquired using the following parameters: TR/TE, 1555/92 ms; slice thickness/gap, 2.0/0.5 mm; matrix, 110 × 110; FOV, 24 × 24 cm²; and four *b* values, 0, 500, 1000, and 1500 s/mm².

IVIM and DKI image analyses

Quantitative parameters including pure molecular diffusion (*D*), pseudo-diffusion coefficient (*D**), perfusion fraction (*f*), mean diffusion (MD), and mean kurtosis (MK) were obtained by processing IVIM and DKI images using MITK software (www.mitk.org). All IVIM and DKI images were independently analyzed by two physicians with more than 5 years of diagnostic experience in abdominal MRI. Final score was the average of the scores obtained by the two observers. Freehand regions of interest (ROIs) were placed in the cortex (CO), the outer medulla (OM), and the inner medulla (IM) using MITK software (Fig. 2).

Statistical analysis

The data were expressed as mean ± standard deviation (SD). One-way analysis of variance (ANOVA) and Tukey’s post hoc test were used for comparisons across multiple groups. Repeated-measure ANOVA and Bonferroni post hoc test for multiple comparisons were

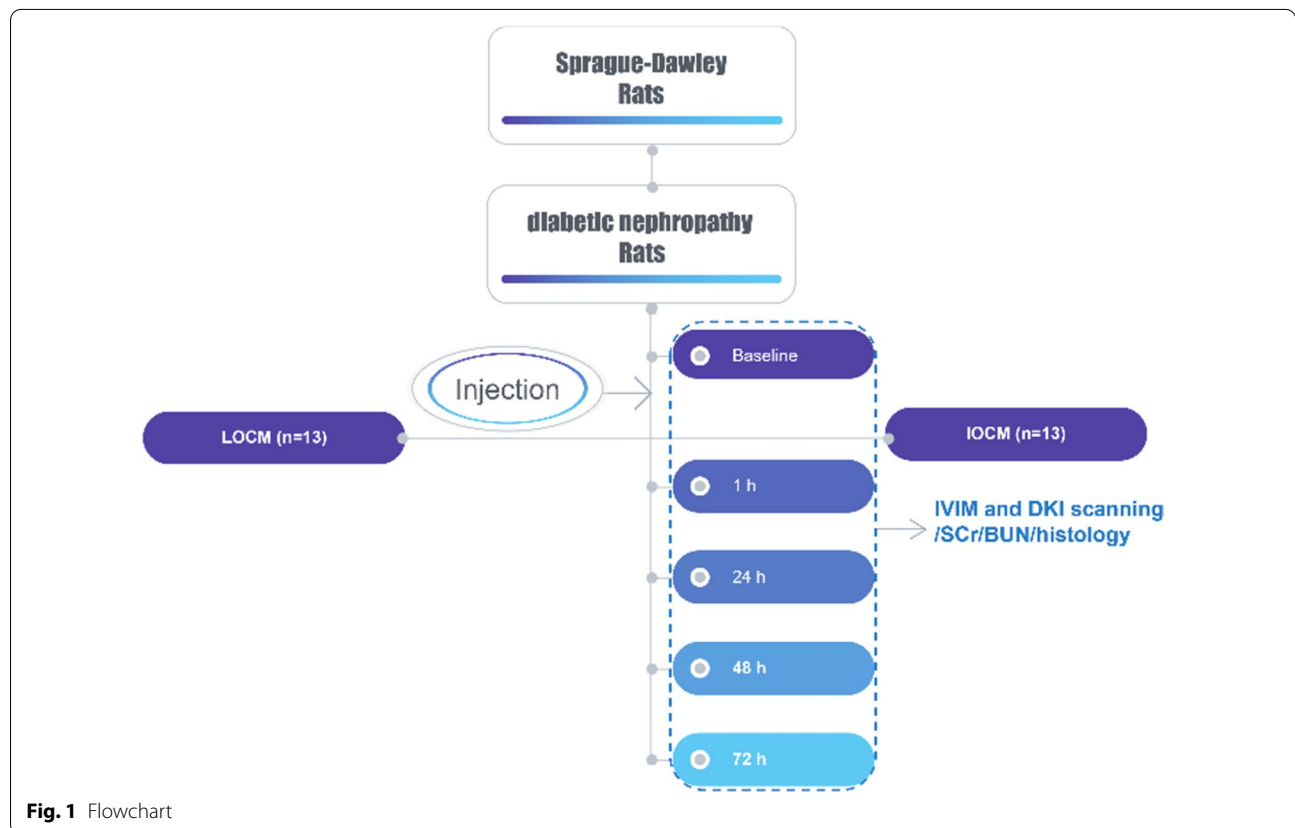
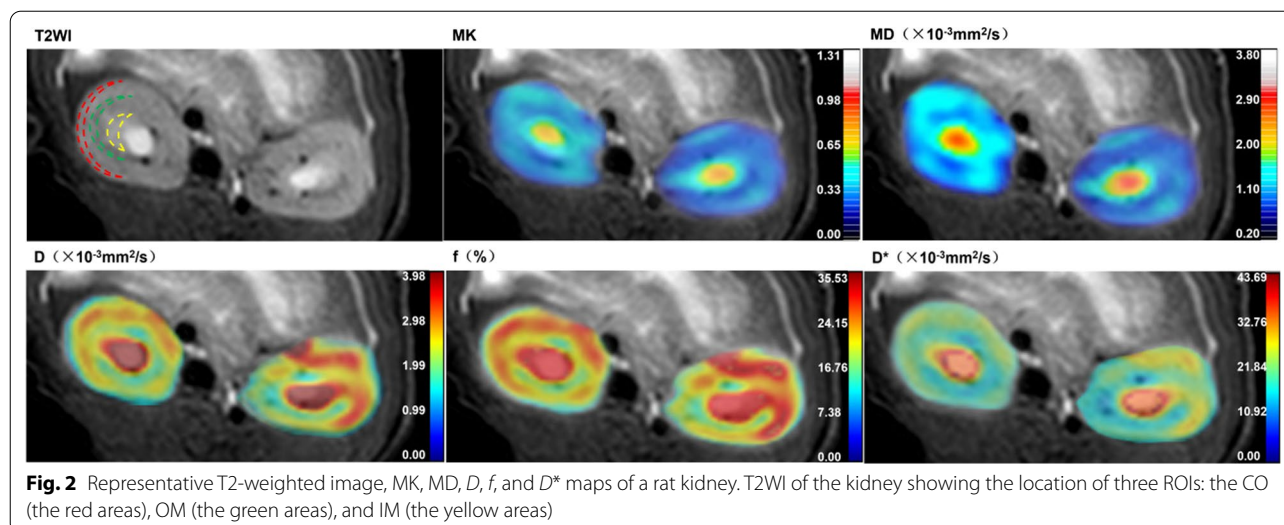


Fig. 1 Flowchart



used to analyze within-group changes of MRI parameters. Correlation analysis between different groups was performed using Spearman's correlation test. Intraclass correlation coefficient (ICC) was used in the analysis of inter-observer agreement between the two radiologists. As given by Bobos et al. [14], an ICC value < 0.40 indicated poor inter-rater agreement; 0.40–0.59 indicated fair agreement; 0.60–0.74 indicated good agreement; and 0.75–1.00 indicated excellent agreement. All statistical analyses were conducted using SPSS version 26.0 (SPSS, Chicago, IL, USA). $p < 0.05$ (two-tailed) indicated a statistical significance.

Results

Progressive changes in IVIM parameters for CI-AKI

Compared against baseline values, D in all renal anatomical compartments decreased in both groups after contrast injection (Table 1 and Fig. 3). D was significantly decreased in the CO and OM of LOCM group ($p = 0.003$ and $p < 0.001$, respectively), and CO and OM of IOCM group ($p = 0.006$ and $p < 0.001$, respectively) 1 h after injection. D was significantly decreased at 48-h in the IM of LOCM and IOCM groups (both $p < 0.001$) compared against the baseline values. Cortical D in the CO of IOCM group reached the lowest level at 48-h ($p < 0.001$) and recovered at 72-h ($p < 0.001$), while the value of the other groups showed a downward trend at 72-h.

Compared against the baseline data, D^* in each anatomical compartment of the kidney was significantly decreased 1 h after injecting contrast agents in both groups (Table 1 and Fig. 3). D^* in each anatomical compartment of LOCM group reached the lowest value at 48-h ($p < 0.001$) and showed an upward trend at 72-h ($p < 0.001$). D^* in each anatomical

compartment of IOCM group reached the lowest value at 24-h ($p < 0.001$) and showed an upward trend at 48-h ($p < 0.001$).

Compared against the baseline levels, f in each anatomical compartment of the kidney was significantly reduced 1 h after contrast injection in both groups (Table 1 and Fig. 3). Cortical f in the CO of LOCM group reached the lowest value at 48-h ($p < 0.001$) and showed a trend of recovery at 72-h ($p < 0.001$). Medullary f in the OM and IM of LOCM group also showed a decreasing trend after 72 h ($p < 0.001$). Additionally, f in each anatomical compartment of IOCM group reached the lowest value at 48-h ($p < 0.001$, $p = 0.039$, and $p = 0.001$, respectively) and showed an increasing trend at 72-h ($p < 0.001$, $p = 0.010$, and $p = 0.113$, respectively).

Progressive changes of DKI parameters for CI-AKI

MD was slightly increased in the OM and IM of the LOCM group ($p = 1.000$), and OM of IOCM group ($p = 1.000$) 1 h after contrast injection compared against baseline values (Table 1 and Fig. 4). MD was slightly decreased in the CO of LOCM group ($p = 1.000$) and CO and IM of IOCM group ($p = 1.000$) at 1-h. After injection of contrast media for 24–72 h, MD in each anatomical compartment was continuously decreased in both groups.

At 1-h after injection, MK was slightly decreased in each anatomical compartment of LOCM group ($p = 0.995$, $p = 0.006$, and $p = 0.570$, respectively) and IOCM group ($p = 1.000$, $p = 0.035$, and $p = 0.617$, respectively) and returned to baseline level at 24–72 h (Table 1 and Fig. 4).

Table 1 Mean IVIM parameters at different time points during the course of CI-AKI

	Group	Baseline	1 h	24 h	48 h	72 h
<i>D</i> ($\times 10^{-3}$ mm ² /s)						
CO	LOCM	1.54 ± 0.10	1.42 ± 0.01*	1.37 ± 0.01*	1.34 ± 0.01*	1.33 ± 0.01*
	IOCM		1.42 ± 0.01*	1.38 ± 0.01*	1.36 ± 0.02*	1.39 ± 0.01*
OM	LOCM	1.55 ± 0.04	1.47 ± 0.04*	1.41 ± 0.01*	1.38 ± 0.15*	1.37 ± 0.01*
	IOCM		1.49 ± 0.01*	1.42 ± 0.01*	1.41 ± 0.08*	1.38 ± 0.01*
IM	LOCM	1.58 ± 0.07	1.48 ± 0.01*	1.38 ± 0.23	1.38 ± 0.01*	1.37 ± 0.01*
	IOCM		1.49 ± 0.01*	1.43 ± 0.01	1.41 ± 0.01*	1.39 ± 0.02*
<i>D*</i> ($\times 10^{-3}$ mm ² /s)						
CO	LOCM	18.55 ± 0.68	12.77 ± 0.16*	10.64 ± 0.02*	9.80 ± 0.05*	10.31 ± 0.26*
	IOCM		13.55 ± 0.29*	11.56 ± 0.28*	12.50 ± 0.25*	12.71 ± 0.20*
OM	LOCM	20.02 ± 0.26	14.83 ± 1.21*	13.15 ± 0.02*	12.33 ± 0.21*	13.50 ± 0.29*
	IOCM		15.65 ± 0.12*	13.87 ± 0.04*	14.50 ± 0.24*	15.05 ± 0.46*
IM	LOCM	19.19 ± 0.31	13.08 ± 0.62*	12.23 ± 1.00*	11.53 ± 0.24*	12.26 ± 0.14*
	IOCM		14.34 ± 0.04*	13.13 ± 0.18*	13.46 ± 0.18*	14.28 ± 0.28*
<i>f</i> (%)						
CO	LOCM	16.80 ± 1.10	14.70 ± 1.22*	12.76 ± 1.64*	11.71 ± 0.60*	12.68 ± 1.27*
	IOCM		14.90 ± 1.46	13.76 ± 1.15*	12.62 ± 0.63*	13.10 ± 0.26*
OM	LOCM	17.16 ± 1.08	15.31 ± 0.83	14.22 ± 1.88*	13.20 ± 1.49*	13.18 ± 1.08*
	IOCM		15.21 ± 2.12*	14.79 ± 1.10*	14.65 ± 1.74*	15.23 ± 0.27*
IM	LOCM	17.12 ± 1.16	15.27 ± 0.95	14.77 ± 2.75	12.33 ± 1.05*	11.69 ± 1.86*
	IOCM		14.31 ± 1.84*	15.25 ± 1.12	13.82 ± 0.91*	14.58 ± 3.05
<i>MD</i> ($\times 10^{-3}$ mm ² /s)						
CO	LOCM	3.20 ± 0.16	3.18 ± 0.03	3.10 ± 0.03	2.86 ± 0.13*	2.76 ± 0.20*
	IOCM		3.19 ± 0.06	2.91 ± 0.006	2.80 ± 0.03*	2.77 ± 0.09*
OM	LOCM	2.29 ± 0.24	2.37 ± 0.02	2.25 ± 0.03	2.06 ± 0.05	1.77 ± 0.10*
	IOCM		2.36 ± 0.17	2.33 ± 0.17	2.26 ± 0.15	1.88 ± 0.07*
IM	LOCM	2.36 ± 0.26	2.39 ± 0.22	2.33 ± 0.24	2.24 ± 0.37	2.24 ± 0.29
	IOCM		2.31 ± 0.24	2.31 ± 0.14	2.11 ± 0.19	2.08 ± 0.24
<i>MK</i>						
CO	LOCM	0.76 ± 0.03	0.74 ± 0.01	0.76 ± 0.04	0.78 ± 0.05	0.85 ± 0.12
	IOCM		0.75 ± 0.06	0.75 ± 0.03	0.76 ± 0.10	0.77 ± 0.09
OM	LOCM	0.81 ± 0.01	0.77 ± 0.02*	0.84 ± 0.04	0.86 ± 0.02	0.90 ± 0.04*
	IOCM		0.78 ± 0.03*	0.82 ± 0.06	0.85 ± 0.08	0.86 ± 0.04
IM	LOCM	0.80 ± 0.14	0.71 ± 0.02	0.72 ± 0.03	0.76 ± 0.10	0.82 ± 0.08
	IOCM		0.71 ± 0.02	0.71 ± 0.04	0.74 ± 0.07	0.78 ± 0.10

*Represents $p < 0.05$ versus baseline

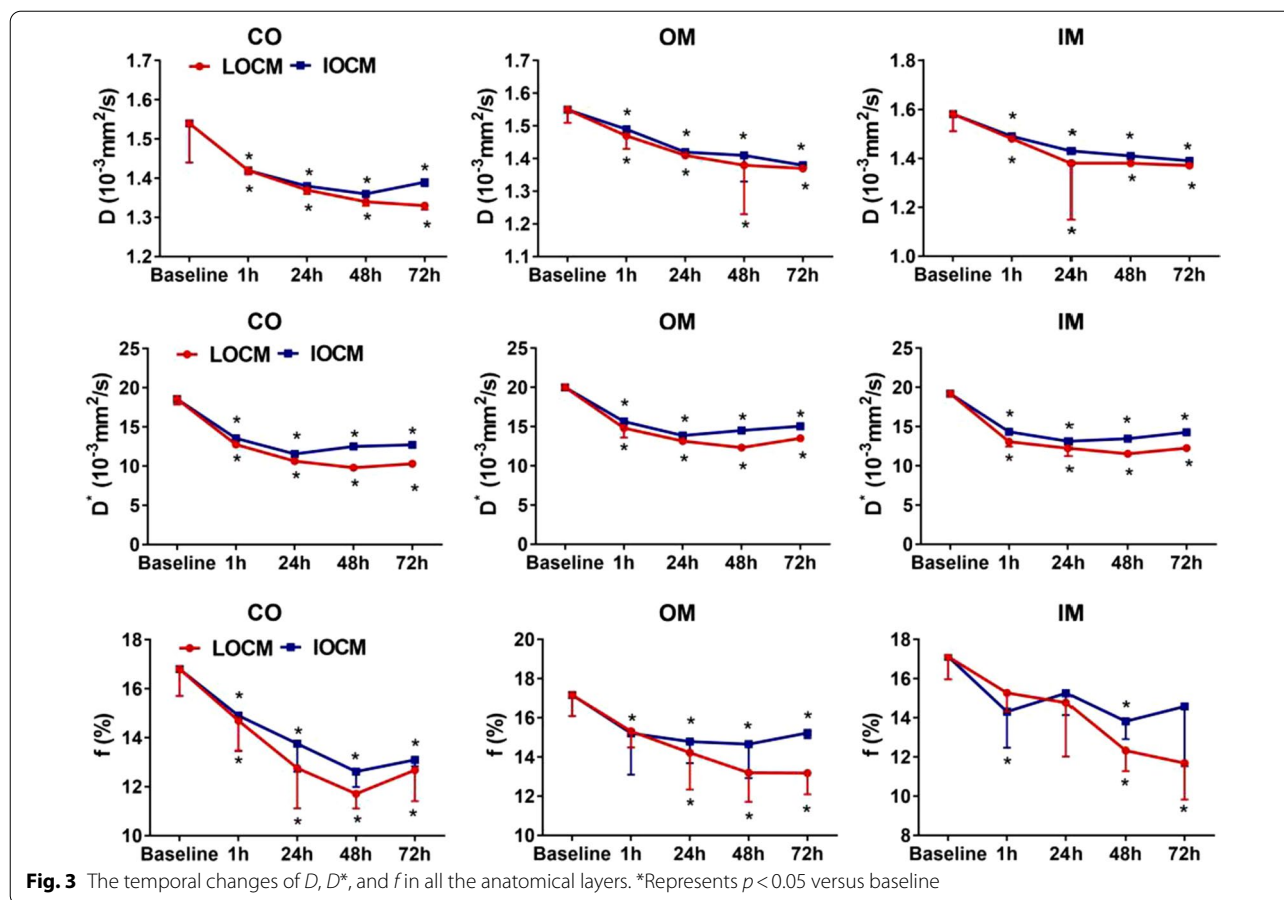
Histological analysis

Pathological sections at each time point showed focal and segmental hyperplasia of glomerular mesangial cells, increased mesangial matrix deposition, disordered arrangement of renal tubular epithelial cells, and cell edema in all DN rats (Fig. 5).

Dilatation of renal tubules, partial swelling of glomerular cells, and hyperemia in the glomerulus were observed 1 h after injection. At 24-h, a large number of erythrocytes were detected in the glomerulus, and abundant lumen proteins were observed in the renal

tubule. At 48-h, degeneration of the glomerular basement membrane and infiltration of inflammatory cells around renal tubules were observed. At 72-h, severe glomerular congestion, degeneration, and cell edema were observed, and urinary proteins were detected in renal tubules.

Compared against baselines, LOCM and IOCM groups showed significantly increased injury scores at 1-, 24-, 48-, and 72-h ($p = 0.012$, $p = 0.010$, $p < 0.001$, and $p < 0.001$; $p = 0.034$, $p = 0.017$, and $p < 0.001$, respectively) (Table 2).



α -SMA immunohistochemistry staining results

The expression level of α -SMA in the renal interstitium of the two groups of rats gradually increased (Fig. 6). Quantitative analysis showed that the difference in α -SMA of the LOCM group against baseline at 48-h and 72-h was statistically significant ($p = 0.006$ and $p = 0.003$, respectively), and the difference comparing the α -SMA of IOCM group against baseline at 72-h was statistically significant ($p = 0.014$) (Table 2).

Blood biomarkers

After injecting contrast agents, SCr and BUN in both groups increased compared to baseline values (Table 3).

Correlation of MRI parameters with pathological scores

As shown in Table 4, a significantly negative correlation was established between kidney injury score and MD in IM. Also, a negative correlation of kidney injury score with D in all anatomical compartments, D^* in all renal anatomical compartments, f in CO and OM, and MD in CO and OM was observed. Kidney injury score showed a low correlation with MK in OM.

Correlation of MRI parameters with α -SMA expression

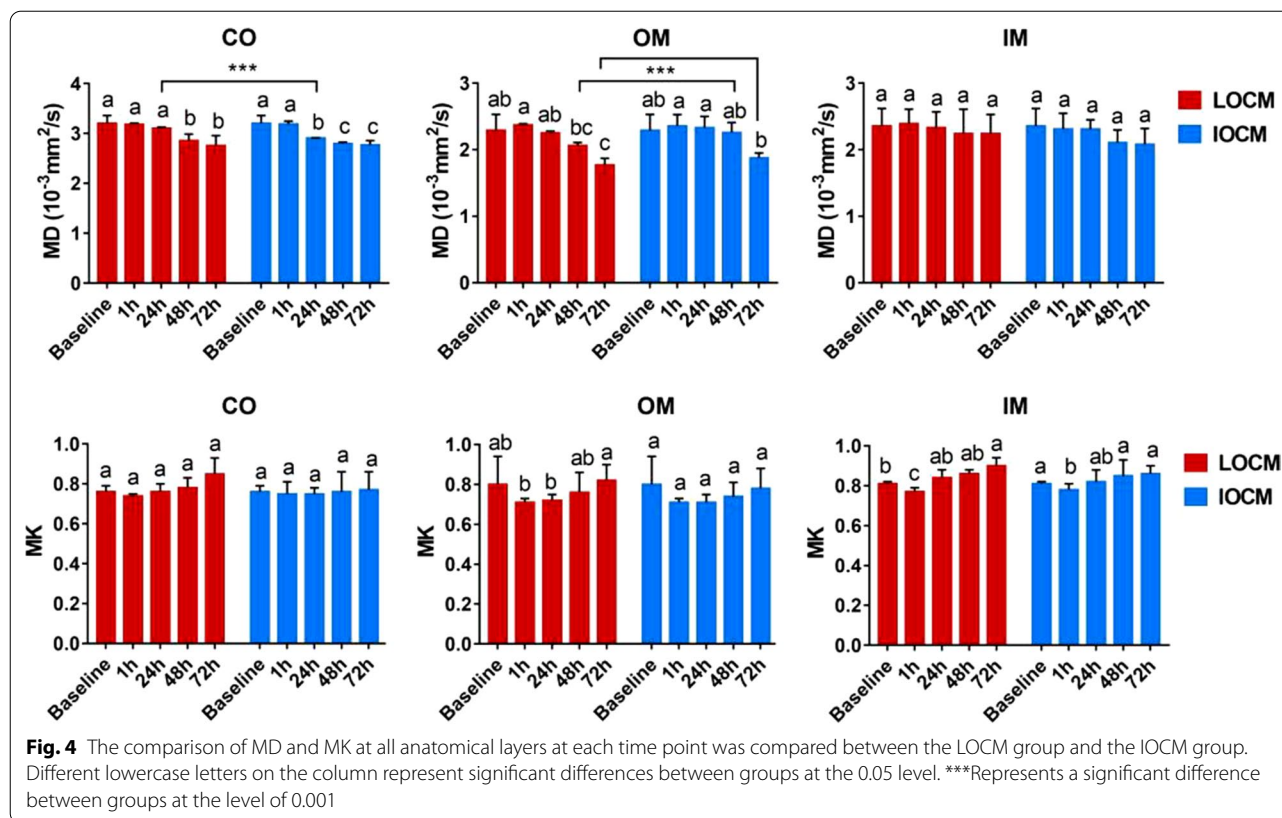
As shown in Table 4, a significantly negative correlation was established between the α -SMA expression level and f in CO, OM, and MD in OM. Also, a good negative correlation of α -SMA expression level with D in all anatomical compartments, D^* in CO and OM, f in IM, and MD in CO and IM was established. The α -SMA expression level showed a low correlation with D^* in IM and MK in OM.

Correlation of MRI parameters with blood biomarkers

As shown in Table 4, a negative correlation of SCr level with D in CO and IM and D^* in all anatomical compartments was established. Also, a negative correlation of SCr level with D in OM, f in all anatomical compartments, and MD in CO and OM was detected. On the other hand, no correlation was established between BUN level and MRI parameters.

Reproducibility

Inter-observer and intra-observer agreements were excellent in all measured quantitative parameters for each anatomical compartment (Table 5).



Discussion

The goal of this study was to compare the adverse effects of LOCM and IOCM on renal water diffusion, perfusion, and tissue microstructure in DN rats diagnosed by IVIM and DKI. MRI findings were substantiated by renal histopathology and α -SMA immunostaining results.

After contrast injection, pure molecular diffusion (D) values in each anatomical compartment of the kidney in both groups decreased gradually from 1 h compared against baseline, indicating contrast-induced renal vascular hypoperfusion [15], which was further verified by H&E staining. Moreover, swollen cells appeared in the proximal convoluted tubules and parts of the glomerulus at the corresponding time points, resulting in increased

resistance to fluid flow in the renal tubules [16]. Another finding was that the lowest values of D in the IOCM group were noted at 48-h in CO and 72-h in IM and OM, and the lowest D values in the LOCM group were recorded at 48-h in CO and 72-h in IM and OM. This phenomenon suggested that the cortex recovered more rapidly than the medulla after kidney injury and that the medulla was highly sensitive to hypoxia [17, 18]. These manifestations led to severe ischemia and hypoxia injury [13], and the recovery time was prolonged.

From 1 h after the injection of contrast agent, the perfusion-related parameters including pseudo-diffusion coefficient (D^*) and perfusion fraction (f) declined gradually, suggesting that the volume of cortical and medulla

Table 2 The change of kidney pathological scores and α -SMA expression scores of DN rat before and after injection of contrast agent

	Group	Baseline	1 h	24 h	48 h	72 h	(F) P
Pathological scores	LOCM	1.02 ± 0.15	1.40 ± 0.14*	1.40 ± 0.13*	1.78 ± 0.15*	1.87 ± 0.14*	(16.049) 0.001
	IOCM		1.27 ± 0.15	1.33 ± 0.10*	1.43 ± 0.12*	1.80 ± 0.14*	(11.235) 0.004
	P	–	0.145	0.341	0.001	0.426	
α -SMA expression scores	LOCM	3.43 ± 0.20	3.79 ± 0.51	3.73 ± 0.51	4.23 ± 0.17*	4.19 ± 0.38*	(8.663) 0.018
	IOCM		3.44 ± 0.18	3.60 ± 0.25	3.73 ± 0.30	4.02 ± 0.26*	(4.721) 0.060
	P	–	0.187	0.642	0.013	0.424	

*Represents $p < 0.05$ versus baseline

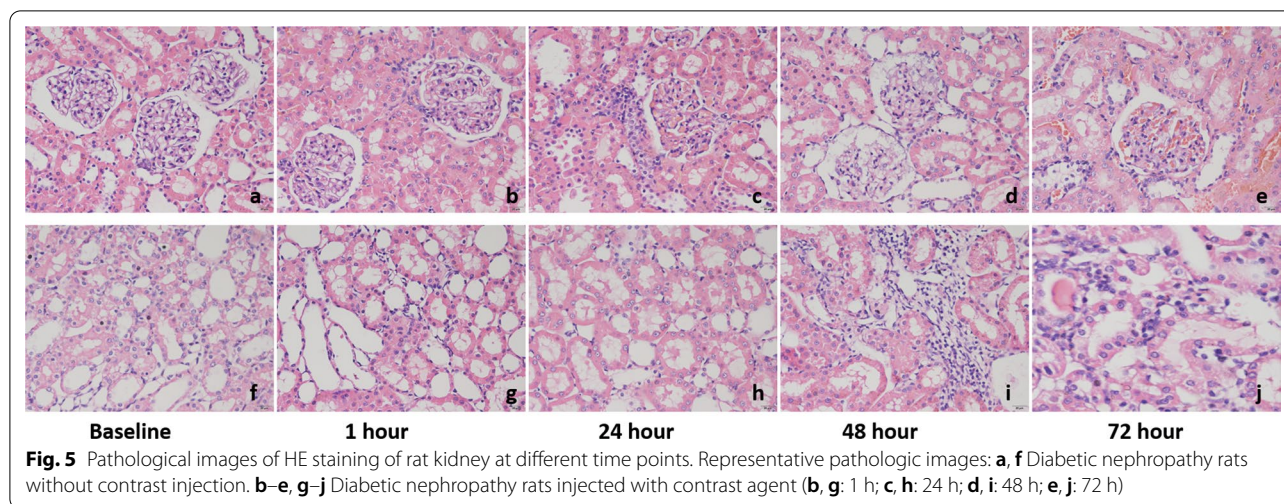


Fig. 5 Pathological images of HE staining of rat kidney at different time points. Representative pathologic images: **a, f** Diabetic nephropathy rats without contrast injection. **b-e, g-j** Diabetic nephropathy rats injected with contrast agent (**b, g**: 1 h; **c, h**: 24 h; **d, i**: 48 h; **e, j**: 72 h)

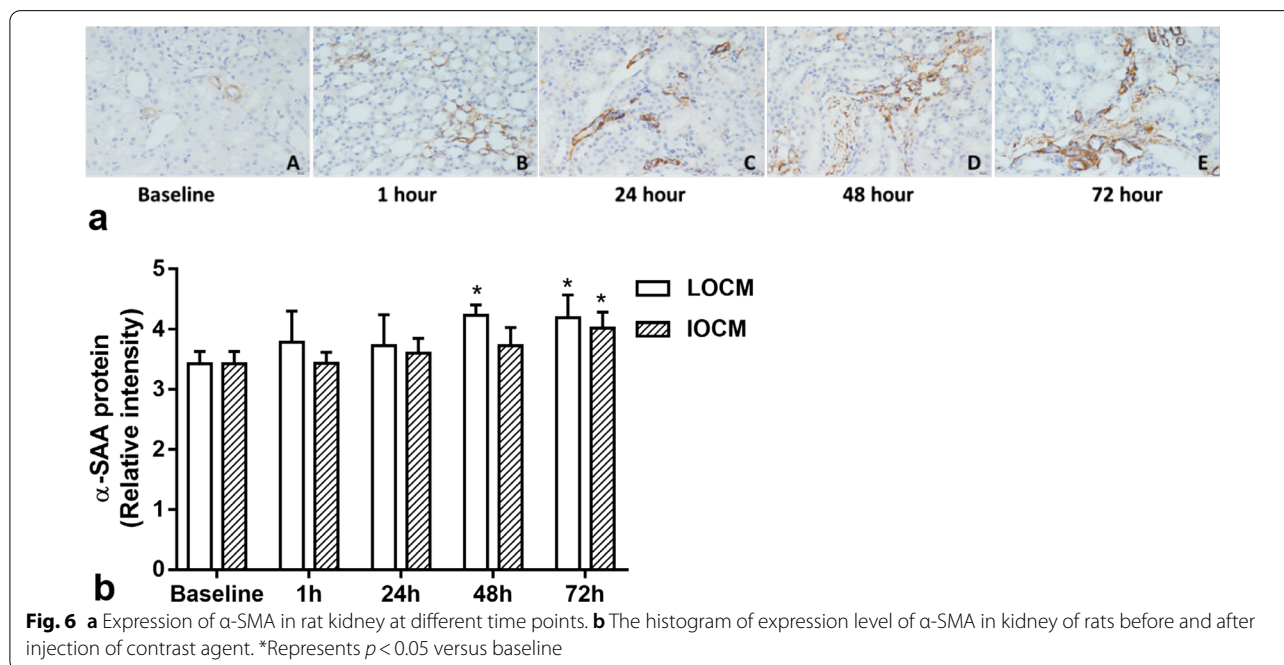


Fig. 6 **a** Expression of α -SMA in rat kidney at different time points. **b** The histogram of expression level of α -SMA in kidney of rats before and after injection of contrast agent. *Represents $p < 0.05$ versus baseline

Table 3 Blood biochemical examinations of DN rats in two groups

Group	Time	SCr ($\mu\text{mol/L}$)	BUN (mmol/L)
LOCM	Baseline	26.69 \pm 2.12	12.66 \pm 2.16
	1 h	27.33 \pm 1.53	12.71 \pm 1.47
	24 h	30.00 \pm 4.00	13.76 \pm 2.65
	48 h	32.67 \pm 4.04	14.96 \pm 3.76*
	72 h	35.00 \pm 3.61*	14.28 \pm 2.77*
IOCM	1 h	27.00 \pm 2.76	13.51 \pm 3.75
	24 h	33.00 \pm 9.54	14.35 \pm 2.45
	48 h	33.67 \pm 2.08	14.57 \pm 1.36
	72 h	28.33 \pm 2.08	12.81 \pm 3.89*

*Represents $p < 0.05$ versus baseline

fluid decreased due to renal tubule response and glomerular vasoconstriction [19]. At 1 h, the decrease in D^* was more obvious than that in f , indicating that vasoconstriction occurred before fluid volume decrease. The recovery time point of D^* was earlier than that of f . Thus, we speculated that the recovery of D^* was related to vascular dilation, and the subsequent increase in f indicated an enlargement in vascular fluid volume (i.e., blood volume) [20], which was caused by vascular dilation. The reason for this mechanism may be that D^* depends largely on vasoconstriction or vasodilatation, while the vasodilatation may increase the capillary pressure, leading to continuous rise of blood volume. Subsequently, with the increase in effective filtration pressure, the capillary

Table 4 Correlation analyses between the MRI parameters and laboratory test index, pathological score, and immunohistochemical expression

Spearman's <i>D</i> ($\times 10^{-3} \text{ mm}^2/\text{s}$) correlation (<i>r, P</i>)	<i>D*</i> ($\times 10^{-3} \text{ mm}^2/\text{s}$)			<i>f</i> (%)			MD ($\times 10^{-3} \text{ mm}^2/\text{s}$)			MK				
	OM	IM	CO	OM	IM	CO	OM	IM	CO	OM	IM	CO	OM	IM
Scr ($\mu\text{mol/L}$)	-0.624, <0.001	-0.448, <0.001	-0.543, <0.001	-0.581, <0.001	-0.515, <0.001	-0.462, <0.001	-0.363, <0.001	-0.315, <0.001	-0.491, <0.001	-0.367, <0.001	-0.169, 0.051	0.118, 0.276, 0.001	0.137, 0.172	0.113
BUN (mmol/L)	-0.234, 0.007	-0.14, 0.11	-0.194, 0.026	-0.216, 0.013	-0.196, 0.025	-0.189, 0.03	-0.15, 0.094	-0.107, 0.233	-0.194, 0.024	-0.094, 0.28	-0.076, 0.384	0.02, 0.089, 0.302	0.822	0.181, 0.036
Pathology scores	-0.784, <0.001	-0.623, <0.001	-0.775, <0.001	-0.674, <0.001	-0.616, <0.001	-0.583, <0.001	-0.510, <0.001	-0.273, 0.002	-0.761, <0.001	-0.576, <0.001	-0.807, <0.001	0.188, 0.452, <0.001	0.268, 0.029	0.002
α -SMA	-0.742, <0.001	-0.617, <0.001	-0.574, <0.001	-0.565, <0.001	-0.543, <0.001	-0.461, <0.001	-0.823, <0.001	-0.707, <0.001	-0.756, <0.001	-0.824, <0.001	-0.737, <0.001	0.153, 0.399, <0.001	0.209, 0.077	0.015

Table 5 Inter-observer and intra-observer reliability estimated by intraclass correlation coefficient (ICC)

	ICC (95% IC)					
	Intra-observer			Inter-observer		
	CO	OM	IM	CO	OM	IM
<i>D</i>	0.956 (0.909–0.979)	0.847 (0.66–0.935)	0.828 (0.634–0.925)	0.961 (0.871–0.989)	0.979 (0.916–0.994)	0.975 (0.919–0.993)
<i>D</i> *	0.979 (0.952–0.991)	0.808 (0.602–0.914)	0.797 (0.578–0.91)	0.996 (0.986–0.999)	0.891 (0.727–0.959)	0.723 (0.236–0.918)
<i>f</i>	0.776 (0.532–0.902)	0.875 (0.738–0.942)	0.810 (0.633–0.906)	0.825 (0.429–0.954)	0.841 (0.514–0.955)	0.978 (0.916–0.994)
MD	0.927 (0.851–0.965)	0.851 (0.704–0.928)	0.826 (0.643–0.919)	0.976 (0.929–0.992)	0.951 (0.855–0.984)	0.918 (0.718–0.978)
MK	0.812 (0.633–0.908)	0.931 (0.851–0.969)	0.939 (0.863–0.974)	0.937 (0.818–0.979)	0.968 (0.902–0.99)	0.753 (0.333–0.923)

All the ICCs reached significant ($p < 0.01$)

blood volume and blood flow of the kidney are gradually restored to the original levels. Thus, the reversion of blood volume could be attributed to the recovery of vasodilation [21, 22]. These findings suggested that parameter *D** was more sensitive than others, which was consistent with the observations by Zhang et al. [23].

MK value in the cortex was lower than that in the ipsilateral medulla. This might be related to the complex structure of the renal medulla, especially renal tubules and collecting tubules, which affected the diffusion limitation of water molecules and made the diffusion distribution deviate from the Gaussian form. This finding was consistent with the previous results by Huang et al. [24]. Cortical MD value was higher than that of ipsilateral medulla, which might be due to fewer diffusion barriers, richer blood perfusion, and more active movement of water molecules in the cortex compared to medulla [10]. When the contrast agent was injected for 1 h, MD in OM in both groups showed an upward trend, and MK in each renal anatomical compartment in both groups showed a downward trend. This phenomenon could be attributed to the direct toxic effect of iodine as a contrast agent, triggering renal tubular necrosis and hindering the diffusion of water molecules, thereby causing tubular structure damage. Simultaneously, the cortical and medullary microstructures were damaged, leading to free diffusion of water molecules, which was deviated from the Gaussian model [25]. At the time point of 24–72 h, MD in each renal anatomical compartment in both groups decreased, and MK increased probably due to inflammatory cell infiltration, leading to fibrous formation [26], limited water molecule diffusion within renal parenchyma, and progressive fibrosis of renal cortex and medulla [27].

The lowest *D* in CO, lowest *D** in each anatomical compartment, and lowest *f* in IM and OM of the IOCM group were detected earlier and greater than those of the LOCM group, suggesting that the renal toxicity in LOCM group was more severe compared with IOCM group, as described previously [28, 29]. In this study, 48 h

after injecting contrast media, the pathological score and the expression level of α -SMA in the LOCM group were distinctly higher than those in the IOCM group (both $p < 0.05$). Combined with MRI findings, the pathological and immunohistochemical analyses suggested that the osmotic pressure of the contrast agent might be the main factor contributing to nephrotoxicity. Long-term nephrotoxicity in the LOCM group was more severe compared with the IOCM group, manifesting as severe renal damage and a higher degree of renal fibrosis in DN rats [30, 31]. This effect might be explained by the fact that the osmotic pressure of the contrast agent became the leading cause of nephrotoxicity under the background condition of DN, and the original foundation of kidney injury accelerated the occurrence and development of comparative kidney injury [32, 33]. Therefore, osmotic pressure exerted a critical influence on renal function in DN patients, and the application of an iso-osmolar contrast medium might be beneficial for these patients.

In addition, the changing trends of parameters in the two groups at other time points were similar, indicating that the mechanism underlying kidney injury induced by two different contrast agents was similar. The current study showed that SCR and BUN were not sensitive indicators of kidney injury, and the changes in *D*, *D**, *f*, MD, and MK occurred much earlier than the changes in blood SCR and BUN [7]. Herein, we observed that most of the IVIM and DKI parameters were correlated with SCR, pathological score, and α -SMA expression. Therefore, we speculated that IVIM and DKI were effective tools in differentiating the changes in renal microcirculation and diagnosing CI-AKI.

In the present study, no significant correlation was established between certain MRI parameters and the two laboratory indexes. This might be due to slight pathological alterations of the tissue structure in early CI-AKI and strong renal compensatory ability, which were not sufficient to cause significant changes in the corresponding laboratory examination results.

Nevertheless, the current study had some limitations. First, the influence of viscosity on renal structure and function was not excluded. Therefore, in future studies, we shall focus on the effect of contrast media viscosity on renal function. Second, the observation period was relatively short, and long-term effects of the contrasts on kidney of diabetic nephropathy could be different. Third, there was no normal control group of animals without injection included. However, this limitation did not influence our observations.

In conclusion, most parameters of IVIM and DKI were significantly correlated with the pathological score and α -SMA expression level. Thus, IVIM and DKI might reflect the effects of iodinated contrast media with a different osmolarity on renal water diffusion, perfusion, and tissue microstructure.

Abbreviations

CI-AKI: Contrast-induced acute kidney injury; DKI: Diffusion kurtosis imaging; DN: Diabetic nephropathy; IOCM: Iso-osmolar contrast medium/media; IVIM: Intravoxel incoherent motion; LOCM: Low-osmolar contrast medium/media; ROI: Region of interest; TE: Echo time; TR: Repetition time.

Acknowledgements

The authors thank Ms. Lijuan Yang for excellent technical assistance.

Author contributions

JS and HD conceived and designed the study. HD, JS, CZ, JL, YX, and RL were involved in the literature search and data collection. HD and CZ analyzed the data. HD and JS wrote the paper. SX, QH, WS, and YY reviewed and edited the manuscript. All authors contributed to the article and approved the submitted version. All authors read and approved the final manuscript.

Funding

Funding was supported by The Endocrine Clinical Medical Center of Yunnan Province (Project NO. ZX20190202); the Fund of the Diabetic Innovation Team in Yunnan Province (Project NO. 2019HC002); the Natural Science Foundation of China (Project NO. 81760734; NO. 31660313; NO. 82160159); and the SKY Image Research Fund, China, (Project NO. Z-2014-07-2003-12).

Availability of data and materials

All data and materials are available within the article.

Declarations

Ethics approval and consent to participate

Ethics approval was obtained from the Ethics Committee of Yunan Medical University (No. YNUCARE20210070).

Consent for publication

Written informed consent for publication was obtained from all participants.

Competing interests

The authors declare no competing interests.

Author details

¹Department of Radiology, The Affiliated Hospital of Yunnan University, NO.176 Qingnian Road, Kunming 650021, Yunnan, China. ²Department of Endocrinology and Metabolism, The Affiliated Hospital of Yunnan University, Kunming, Yunnan, China. ³Department of Hospital Quality Control, The Affiliated Hospital of Yunnan University, Kunming, Yunnan, China.

Received: 7 February 2022 Accepted: 7 June 2022

Published online: 29 June 2022

References

- Werner S, Bez C, Hinterleitner C, Horger M (2020) Incidence of contrast-induced acute kidney injury (CI-AKI) in high-risk oncology patients undergoing contrast-enhanced CT with a reduced dose of the iso-osmolar iodinated contrast medium iodixanol. *PLoS One* 15(5):e0233433. <https://doi.org/10.1371/journal.pone.0233433>
- Mamoulakis C, Tsarouhas K, Fragkiadoulaki I et al (2017) Contrast-induced nephropathy: basic concepts, pathophysiological implications and prevention strategies. *Pharmacol Ther* 180:99–112. <https://doi.org/10.1016/j.pharmthera.2017.06.009>
- Tan H, Yi H, Zhao W, Ma JX, Zhang Y, Zhou X (2016) Intraglomerular cross-talk elaborately regulates podocyte injury and repair in diabetic patients: insights from a 3D multiscale modeling study. *Oncotarget* 7(45):73130–73146. <https://doi.org/10.18632/oncotarget.12233>
- Bartel DP (2004) MicroRNAs: genomics, biogenesis, mechanism, and function. *Cell* 116(2):281–297. [https://doi.org/10.1016/s0092-8674\(04\)00045-5](https://doi.org/10.1016/s0092-8674(04)00045-5)
- Vallon V (2011) The proximal tubule in the pathophysiology of the diabetic kidney. *Am J Physiol Regul Integr Comp Physiol* 300(5):R1009–R1022. <https://doi.org/10.1152/ajpregu.00809.2010>
- Khawaja S, Jafri L, Siddiqui I, Hashmi M, Ghani F (2019) The utility of neutrophil gelatinase-associated lipocalin (NGAL) as a marker of acute kidney injury (AKI) in critically ill patients. *Biomark Res*. 7:4. <https://doi.org/10.1186/s40364-019-0155-1>
- Liang L, Chen WB, Chan KW et al (2016) Using intravoxel incoherent motion MR imaging to study the renal pathophysiological process of contrast-induced acute kidney injury in rats: comparison with conventional DWI and arterial spin labelling. *Eur Radiol* 26(6):1597–1605. <https://doi.org/10.1007/s00330-015-3990-y>
- Wang Y, Zhang X, Hua Z et al (2019) Blood oxygen level-dependent imaging and intravoxel incoherent motion MRI of early contrast-induced acute kidney injury in a rabbit model. *Kidney Blood Press Res* 44(4):496–512. <https://doi.org/10.1159/000500052>
- Pentang G, Lanzman RS, Heusch P et al (2014) Diffusion kurtosis imaging of the human kidney: a feasibility study. *Magn Reson Imaging* 32(5):413–420. <https://doi.org/10.1016/j.mri.2014.01.006>
- Zhou H, Zhang J, Zhang XM et al (2020) Non-invasive evaluation of early diabetic nephropathy using diffusion kurtosis imaging: an experimental study. *Eur Radiol*. <https://doi.org/10.1007/s00330-020-07322-6>
- Liu Y, Zhang GM, Peng X et al (2018) Diffusional kurtosis imaging in assessing renal function and pathology of IgA nephropathy: a preliminary clinical study. *Clin Radiol* 73(9):818–826. <https://doi.org/10.1016/j.crad.2018.05.012>
- Sharma G, Ashhar MU, Aeri V et al (2019) Development and characterization of late-stage diabetes mellitus and -associated vascular complications. *Life Sci* 216:295–304
- Wang JH, Ren K, Sun WG, Zhao L, Zhong HS, Xu K (2014) Effects of iodinated contrast agents on renal oxygenation level determined by blood oxygenation level dependent magnetic resonance imaging in rabbit models of type 1 and type 2 diabetic nephropathy. *BMC Nephrol* 15:140. <https://doi.org/10.1186/1471-2369-15-140>
- Bobos P, MacDermid J, Nazari G, Furtado R, CATWAD (2019) Psychometric properties of the global rating of change scales in patients with neck disorders: a systematic review with meta-analysis and meta-regression. *BMJ Open* 9(11):e033909. <https://doi.org/10.1136/bmjopen-2019-033909>
- Rheinheimer S, Schneider F, Stieltjes B et al (2012) IVIM-DWI of transplanted kidneys: reduced diffusion and perfusion dependent on cold ischemia time. *Eur J Radiol* 81(9):e951–e956. <https://doi.org/10.1016/j.ejrad.2012.06.008>
- Wang Z, Liu H, Meng H, Zhang D (2020) Application of diffusion tensor imaging and blood oxygenation level-dependent magnetic resonance imaging to assess bilateral renal function induced by Iohexol in rabbits. *BMC Nephrol* 21(1):210. <https://doi.org/10.1186/s12882-020-01857-y>

17. Wybraniec MT, Mizia-Stec K, Więcek A (2015) Contrast-induced acute kidney injury: the dark side of cardiac catheterization. *Pol Arch Med Wewn* 125(12):938–949. <https://doi.org/10.20452/pamw.3218>
18. Li LP, Lu J, Franklin T, Zhou Y, Solomon R, Prasad PV (2015) Effect of iodinated contrast medium in diabetic rat kidneys as evaluated by blood-oxygenation-level-dependent magnetic resonance imaging and urinary neutrophil gelatinase-associated lipocalin. *Invest Radiol* 50(6):392–396. <https://doi.org/10.1097/RLI.000000000000141>
19. Stefanska A, Eng D, Kaverina N et al (2016) Cells of renin lineage express hypoxia inducible factor 2 α following experimental ureteral obstruction. *BMC Nephrol* 17:5. <https://doi.org/10.1186/s12882-015-0216-0>
20. Sigmund EE, Vivier PH, Sui D et al (2012) Intravoxel incoherent motion and diffusion-tensor imaging in renal tissue under hydration and furosemide flow challenges. *Radiology* 263(3):758–769. <https://doi.org/10.1148/radiol.12111327>
21. Leong CL, Anderson WP, O'Connor PM, Evans RG (2007) Evidence that renal arterial-venous oxygen shunting contributes to dynamic regulation of renal oxygenation. *Am J Physiol Renal Physiol* 292(6):F1726–F1733. <https://doi.org/10.1152/ajprenal.00436.2006>
22. Yan YY, Hartono S, Hennedige T et al (2017) Intravoxel incoherent motion and diffusion tensor imaging of early renal fibrosis induced in a murine model of streptozotocin induced diabetes. *Magn Reson Imaging* 38:71–76. <https://doi.org/10.1016/j.mri.2016.12.023>
23. Zhang B, Dong Y, Guo B et al (2018) Application of non-invasive functional imaging to monitor the progressive changes in kidney diffusion and perfusion in contrast-induced acute kidney injury rats at 3.0 T. *Abdom Radiol (NY)*. 43(3):655–662. <https://doi.org/10.1007/s00261-017-1247-8>
24. Huang Y, Chen X, Zhang Z et al (2015) MRI quantification of non-Gaussian water diffusion in normal human kidney: a diffusional kurtosis imaging study. *NMR Biomed* 28(2):154–161. <https://doi.org/10.1002/nbm.3235>
25. Li A, Liang L, Liang P et al (2020) Assessment of renal fibrosis in a rat model of unilateral ureteral obstruction with diffusion kurtosis imaging: comparison with α -SMA expression and 18F-FDG PET. *Magn Reson Imaging* 66:176–184. <https://doi.org/10.1016/j.mri.2019.08.035>
26. Wang Y, Zhang X, Wang B et al (2019) Evaluation of renal pathophysiological processes induced by an iodinated contrast agent in a diabetic rabbit model using intravoxel incoherent motion and blood oxygenation level-dependent magnetic resonance imaging. *Korean J Radiol* 20(5):830–843. <https://doi.org/10.3348/kjr.2018.0757>
27. Tervaert TW, Mooyaart AL, Amann K et al (2010) Pathologic classification of diabetic nephropathy. *J Am Soc Nephrol*. 21(4):556–563. <https://doi.org/10.1681/ASN.2010010010>
28. Jensen H, Doughty RW, Grant D, Myhre O (2011) The effects of the iodinated X-ray contrast media iodixanol, iohexol, iopromide, and ioversol on the rat kidney epithelial cell line NRK 52-E. *Ren Fail* 33(4):426–433. <https://doi.org/10.3109/0886022X.2011.568146>
29. Hernández F, Mora L, García-Tejada J et al (2009) Comparison of iodixanol and ioversol for the prevention of contrast-induced nephropathy in diabetic patients after coronary angiography or angioplasty. *Rev Esp Cardiol* 62(12):1373–1380. [https://doi.org/10.1016/s1885-5857\(09\)73531-5](https://doi.org/10.1016/s1885-5857(09)73531-5)
30. McCullough PA (2008) Radiocontrast-induced acute kidney injury. *Nephron Physiol* 109(4):p61–72. <https://doi.org/10.1159/000142938>
31. McCullough PA, Bertrand ME, Brinker JA, Stacul F (2006) A meta-analysis of the renal safety of isosmolar iodixanol compared with low-osmolar contrast media. *J Am Coll Cardiol* 48(4):692–699. <https://doi.org/10.1016/j.jacc.2006.02.073>
32. Poh WY, Omar MS, Tan HP (2018) Predictive factors for contrast-induced acute kidney injury in high-risk patients given *N*-acetylcysteine prophylaxis. *Ann Saudi Med* 38(4):269–276. <https://doi.org/10.5144/0256-4947.2018.269>
33. Fernandes SM, Martins DM, da Fonseca CD, Watanabe M, Vattimo MF (2016) Impact of iodinated contrast on renal function and hemodynamics in rats with chronic hyperglycemia and chronic kidney disease. *Biomed Res Int* 2016:3019410. <https://doi.org/10.1155/2016/3019410>

Publisher's Note

Springer Nature remains neutral with regard to jurisdictional claims in published maps and institutional affiliations.

Submit your manuscript to a SpringerOpen[®] journal and benefit from:

- Convenient online submission
- Rigorous peer review
- Open access: articles freely available online
- High visibility within the field
- Retaining the copyright to your article

Submit your next manuscript at ► [springeropen.com](https://www.springeropen.com)
